PROCEEDINGS, 49th Workshop on Geothermal Reservoir Engineering
Stanford University, Stanford, California, February 12-14, 2024
SGP-TR-227

Major and Trace Elements Geochemistry of Natural Waters at Mt. Meru Volcano, Tanzania

Sadock Josephat, Andri Stefánsson and Finnbogi Óskarsson

Tanzania Geothermal Development Company Ltd, P. O Box 14801 Dar es Salaam

E-mail address: *sadockz16@gmail.com*

Keywords: Tanzania, Mt. Meru volcano, EARS, major elements, geothermal, elemental mobility

ABSTRACT

The geochemistry of natural waters at Mt. Meru volcano in northern Tanzania was studied. The study area of the present study is on the eastern side of Mt. Meru volcano and lies at an elevation of 1230 to 4565 meters above sea level. It is in the volcanic province of northern Tanzania, in the Gregory Rift of the East Africa Rift System. In the study area, processes controlling the composition of major and trace elements, and mobility of various elements in thermal and non-thermal waters are not well understood. This study was intended to investigate the geochemistry of major and trace elements in the ground-, surface- and lake waters at Mt. Meru volcano. It focuses on the origin of the waters and processes affecting water composition, mobility of major and trace elements, and characterization of end-member water sources. The study involved sampling and analysis of spring-, stream-, river-, lake-, and groundwaters. PHREEQC was used for the calculation of aqueous speciation and mineral saturation indices. Results suggest that the studied waters are of meteoric origin as indicated by δ^2H-H_2O and $\delta^{18}O$-H_2O, with Na-HCO_3 composition. The chemistry of the studied waters is mainly controlled by the progressive dissolution of rocks at relatively low temperatures as indicated by the correlation between major constituents (Na, K, Mg, SO_4, and Cl).

Two possible end-member water compositions, namely non-reacted rainwater and reacted water have been identified in this study. The composition of most of the studied waters fall between these two end members. The saline lakes are formed by evaporation of waters sourced in the higher altitudes of Mt. Meru volcano, and the high concentration of dissolved constituents is attributed to evaporative concentration. The composition of studied waters is further attributed to dissolution of carbonates, mixing with biogenic and atmospheric CO_2, and input of deep volatiles as suggested based on $\delta^{13}C$-CO_2. The element mobility relative to Na is generally low in the studied waters, suggesting that many elements are incorporated into weathering and hydrothermal alteration minerals. Geothermometry based on multiple mineral equilibria suggests a possible low-temperature geothermal system on the eastern flank of Mt. Meru with a subsurface temperature of <100 °C possibly resulting from the shallow circulation of meteoric water.

1. INTRODUCTION

Geochemical and hydrological factors and processes among others control water composition. For instance water-rock interaction, mixing of waters of variable sources, evaporation and input of deep gases may all contribute to the chemical composition of natural waters (White 2020). Moreover, the chemical and isotope composition of natural waters can provide insight into some of the hydrogeological features of groundwater systems, both thermal and non-thermal systems. For instance the stable isotopes of water (δ^2H and $\delta^{18}O$) can be used to trace the water sources, progressive water-rock interaction and evaporation processes (Allegre, 2008; Sharp, 2017). In addition, non-reactive elements, for example B and Cl, have been used to evaluate the progress of water-rock interaction and mixing of waters of variable origin (e.g., Arnórsson and Andrésdóttir, 1995) whereas the reactive elements, for example Si, Na, K, Ca, Mg, Al and Fe, are incorporated into secondary and weathering minerals (Kaasalainen and Stefánsson, 2012).

Trace element composition of natural waters has received less attention than major element chemistry. Most of the previous studies on trace element chemistry in groundwater systems have focused on their concentrations rather than quantifying the processes controlling their composition. However, such studies (e.g., Kaasalainen and Stefánsson, 2012) have demonstrated that trace elements geochemistry can be quantified in a similar manner as many major elements, i.e., by studying water mixing and water-rock interaction.

Previous hydrogeological and geochemical studies at Mt. Meru volcano (Tanzania) and the surrounding areas have postulated groundwater composition at Mt. Meru to be controlled by the aquifer lithology and climate factors including high precipitation and temperature (Bennett et al., 2022; Makoba and Muzuka, 2019; Tomašek et al., 2022). High precipitation and warm temperature are associated with enhanced dissolution of rocks (e.g., Gislason, 2008). Water hosted in the fractured volcanic rocks, breccia, and tuff formations has lower concentrations of dissolved elements compared to the water hosted in lahars, which are more susceptible to weathering. Moreover, the deep circulating groundwater evinces lower concentrations of dissolved elements than shallow circulating water, attributed to slower

weathering and dissolution rate of aluminosilicate minerals composing the deep aquifer than the pyroclastic deposits that form the shallower aquifers (Bennett et al., 2021). In contrast the geochemistry of trace elements is not well understood as well as the mobility of various elements, both in thermal and non-thermal waters.

The purpose of this study is to investigate the geochemistry of major and trace elements in the ground-, surface- and lake waters at Mt. Meru volcano. It focuses on the origin of the waters and processes affecting water composition, mobility of major and trace elements, and characterization of end-member water sources.

2. STUDY AREA

2.1 Geological Background

Mt. Meru is a stratovolcano in the eastern branch (Gregorian rift) of the East Africa Rift System (EARS). This rift extends from northeast of Africa in the Gulf of Aden to eastern Africa in Mozambique (Figure 2- 1). The EARS is observed as a succession of basins bordered by the uplifted blocks while the central part is subsiding, and it has two main branches: the eastern and the western branches. The Gregory rift extends from the Gulf of Aden to Ethiopia and Kenya and ends in the rift basins of the northern Tanzania volcanic zone (Chorowicz, 2005; Mahecha, 2019). High relief areas in the EARS corresponds to the Ethiopian dome, Kenyan dome and Tanzanian dome (Chorowicz, 2005) and are attributed to volcanism, tectonic belts, and graben shoulders. The eastern branch has more volcanic activity than the western branch and is believed to have more geothermal potential. The propagation of the EARS is attributed to the rising mantle plume (Delcamp et al., 2013). This plume has been detected by gravity and seismic imaging and also indicated by the noble gases provenance (Halldórsson et al., 2014). The formation of domes, upper mantle thinning, intrusion and thermal uplift is analogue to early stage of passive continental margin preceding opening of an ocean (Chorowicz, 2005).

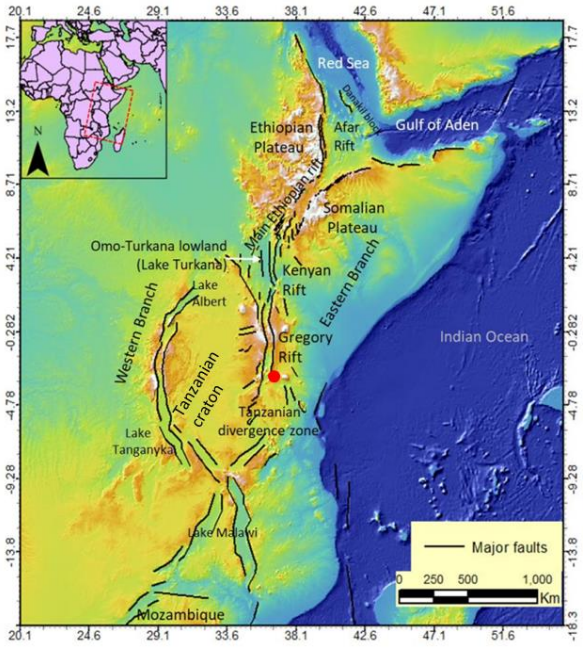

Figure 2- 1: Digital elevation map of the Eastern Africa showing the East African Rift System (EARS) (Kebede, 2021). The location of the study area is indicated by the red dot.

Volcanoes in the Northern Tanzania Divergence Zone (NTDZ) occur in alignments which can be correlated to the rift structures, and the recognized trends are the N-S, the NE-SW and NW-SE. Other trends are the ENE-WSW evidenced by the alignment of Ngorongoro-Monduli-Meru-Kilimanjaro volcanoes (Figure 2- 2) (Delcamp et al., 2013; Le Gall et al., 2008). This suggest that magmatism in the NTDZ is structural controlled. Volcanic activity in the northern Tanzania is younger than its northern counterparts in Kenya and Ethiopia (Chorowicz, 2005; Dawson, 1992), suggesting southern migration of the mantle plume (Dawson, 2008; Roberts, 2002). Alkaline volcanism in Meru occurred in hiatus, the early events were 2.0–1.5 Ma followed by other events 0.35-0.16 Ma (Roberts, 2002; Wilkinson

et al., 1986). The main Meru cone building eruption occurred 0.16-0.06 Ma followed by small events which were observed until the 20th century (Wilkinson et al., 1986). The last documented eruption at Mt. Meru volcano occurred at ash cone in 1910 and produced black ash at the top of ash cone (Delcamp et al., 2013; Ghiglieri et al., 2010; Wilkinson et al., 1986) which is a resurgent volcano erupted after the collapse of the main Meru cone on its eastern flank.

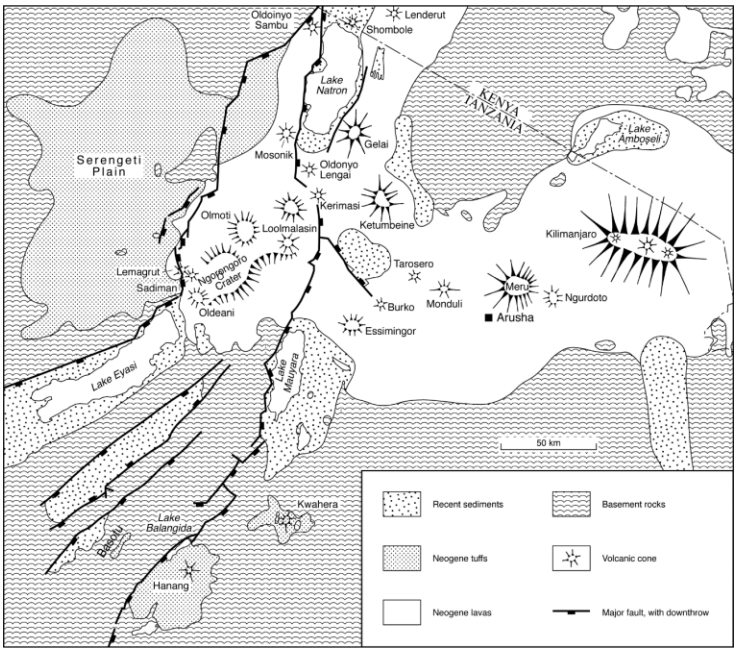

Figure 2- 2: Map showing volcanoes and tectonic lineament in the Northern Tanzania Divergence Zone (Foster et al., 1997).

The surface geology is dominated by volcanics (Figure 2- 3), and volcanic tuffs are distributed throughout the northern volcanic province of Tanzania (Dawson, 1992). Other rock units include basaltic lava flows, nephelinite, pyroclastic deposits, and volcanic breccia which contain phonolite clasts associated with Meru and Ngurdoto crater eruptions (Roberts 2002). Debris avalanche characterized by presence of large boulders within fine matrix which is a result of collapse of the Mt. Meru volcano, cover a large area on the eastern flank. The main cone of Meru is peralkaline trachyte, phonolites and nephelinites while carbonatite lava and pyroclactics occur with nepheline at Oldoinyo Lengai, Hanang, Kwaraha and Kerimasi (Dawson, 1992). Mt. Meru volcano collapsed on its eastern flank ~7800 years ago resulting in a lahar covering an area of ~1500 km^2 to the northeast, east and southeast of the volcano up to the foot of Mt. Kilimanjaro volcano (Wilkinson et al., 1986). This wide spread of lahar was aided by the presence of large quantity of water that acted as lubricant (Delcamp et al., 2016) and was followed by construction of lava dome and ash cone in the 3.5 km diameter Meru crater on the eastern flank of the volcano (Roberts, 2002; Wilkinson et al., 1986).

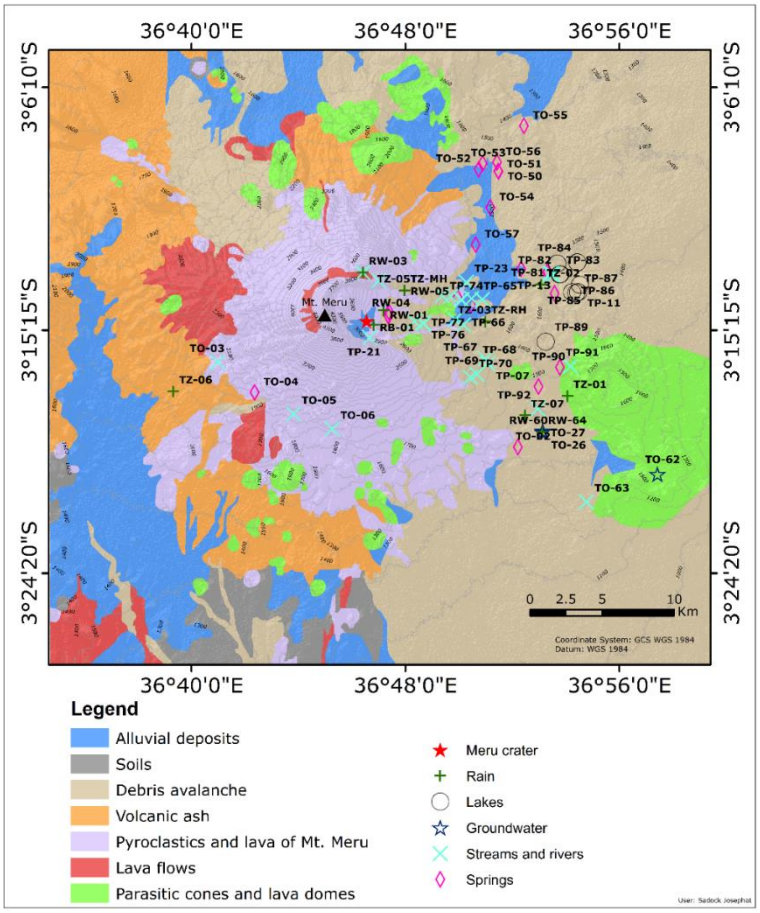

Figure 2- 3: Geological map of Mt. Meru volcano area modified from Tomašek et al. (2022). The locations of sampling sites in the present study are also indicated.

2.2 Hydrogeology

Hydrology in the area is influenced by Mt. Meru volcano. The drainage system is radial from higher to lower elevation with streams and rivers, while lakes occur only to the eastern side of the volcano (Figures 2-3 and 5-7). Water flow is complicated by tectonic structures such as grabens, faults, eruptive activity, lava domes, vegetation cover, thermal regime, and tholoids (Delcamp et al., 2016; Ghiglieri et al., 2010). The hydrological model of Mt. Meru volcano can be explained as the typical mature volcano where aquifers developed at temperate conditions when recharge was higher than discharge (Delcamp et al., 2016). The collapse of Meru volcano, which cut one third of the volcano, disrupted the aquifer leading to loss of large quantity of stored water and this water acted as a lubricant for lahar flow (Delcamp et al., 2013). However, the aquifer may have redeveloped following the post collapse eruption leading to emplacement of ash cone in the collapse scur.

Water flow in the area has been categorized into local, intermediate, and regional flow systems by Bennett et al. (2021). The regional flow system has been regarded as deeper with longer residence time while the local and intermediate flow are shallow with short residence time (**Error! Reference source not found.**). However, controls of the water composition and mixing trends between different endmembers were not well established and are described in this study.

2.3 Geothermal Activity

The northern volcanic province of Tanzania is characterized by various geothermal activity like thermal springs, deposits, and mineral alteration. Thermal springs in this zone indicate great variability in discharge temperatures and chemical composition between specific

prospect areas. The known discharge temperatures range from 20 °C to 71 °C, pH from 7.4 to 10, and composition ranging from Na-Cl to Na-HCO3 waters. At Mt. Meru fumarolic activity was observed after the 1910 ash cone eruption but vanished after 1954 (Ghiglieri et al., 2010; Wilkinson et al., 1986). At present, the evidence of this fumarolic activity is presented by fossil argillic alteration observed at the ash cone. High heat flux in the order of 90-104 mW/m^2 has been identified in the Northern Tanzania Divergence Zone by Didas et al. (2022).

The Njekukumia springs located at high elevation and in thick vegetation cover, indicates high dissolved solute content compared to other springs in the area. A few other springs at lower elevation on the eastern and north-eastern flanks of Mt. Meru volcano display similar composition as the Njekukumia springs including springs in the Lendoiya and Ngarenayuki villages. Such high content of dissolved elements may be signs of thermal water input. However, the geothermal activity at Mt. Meru is poorly characterized and in fact mostly unknown. Reservoir temperatures in the range of 50 - 90 °C have been estimated based on geothermometry with water circulation depth down to ~1.5 km assuming a geothermal gradient of 45 °C/km (Bennett, 2022) and <100 °C by Josephat 2023. Alteration minerals identified in Meru include ferric oxide, alunite, calcite, and kaolinite. Analysis of rock and soil samples confirmed the occurrence of alunite together with levynite, K-feldspars, hematite and halloysite (Mahecha, 2019). Native sulfur, which is commonly observed in association with steam-heated acid-sulfate waters was observed at the ash cone. Most of these alteration minerals were observed in the Meru crater and the peak of ash cone and are typical mineralogy associated with argillic alteration (Mahecha, 2019; Mahecha et al., 2021).

3. METHODS

3.1 Sampling and Analysis

Water samples were collected on the upper flanks of Mt. Meru volcano in 2017, in total 64 samples of springs, streams, rivers, lakes, and groundwater. Rainwater was also collected from different locations in the Arusha National Park and outside the park (Figure 2- 3). On-site measurements of water temperature, pH, EC, and redox potential (ORP) were conducted using a WTW Multimeter. The pH was measured by a combination pH electrode inbuilt in a multimeter and was calibrated using 4.0, 7.0 and 10.0 buffer solutions whereas the EC electrode was calibrated using KCl solution. Water samples were collected for the analysis of anions (F, Cl, Br, ΣCO_2, SO_4, NO_3 and PO_4), major and trace cations (Na, K, Ca, Mg, Si, Al, Fe, B, Sr, As, Ba, Be, Bi, Cd, Ce, Co, Cr, Cs, Cu, Dy, Er, Eu, Ga, Gd, Ge, Hf, Hg, Ho, In, La, Li, Lu, Mn, Mo, Nb, Nd, Ni, Pb, Pr, Rb, Sb, Sc, Se, Sm, Sn, Sr, Ta, Tb, Te, Th, Ti, Tl, Tm, U, V, W, Y, Yb, Zn, and Zr), and selected stable isotope ratios (δ^2H-H_2O, δ^{18}O-H_2O, and δ^{13}C-CO_2).

Samples for analysis of anions were collected into polyethylene (PE) bottles with no further sample treatment. Samples for analysis of cations (major and trace) were filtered using PE syringes fitted with disposable 0.45 µm cellulose acetate filters, collected in PE bottles and acidified with 1 mL ultrapure 65% HNO_3 in 100 mL sample. Samples for analysis of stable water isotopes (δ^2H-H_2O and δ^{18}O-H_2O) were collected in brown glass bottles with double stoppers. Samples for analysis of δ^{13}C-CO_2 were filtered using PE syringes fitted with disposable 0.45 µm cellulose acetate filters and collected into glass bottles with no further treatment. The water samples were analyzed at the Groundwater Resources, Soil as a Resource and Resource Geochemistry laboratories of Federal Institute for Geosciences and Natural Resources (BGR) in Hanover, Germany. The concentrations of anions (F, Cl, Br, SO_4, ΣCO_2, PO_4, and NO_3) were determined by ion chromatography (Dionex-2000). Major cations (Na, K, Mg, Ca, Si, Fe, Al) were analyzed using Spectro Arcos Inductively Coupled Plasma Optical Emission Spectroscopy (ICP-OES) while trace elements (B, Sr, As, Ba, Be, Bi, Cd, Ce, Co, Cr, Cs, Cu, Dy, Er, Eu, Ga, Gd, Ge, Hf, Hg, Ho, In, La, Li, Lu, Mn, Mo, Nb, Nd, Ni, Pb, Pr, Rb, Sb, Sc, Se, Sm, Sn, Sr, Ta, Tb, Te, Th, Ti, Tl, Tm, U, V, W, Y, Yb, Zn, and Zr) were determined using Agilent 7800 Inductively Coupled Plasma Mass Spectrometry (ICP-MS). Determination of δ^2H-H_2O and δ^{18}O-H_2O was done using Picarro L2130-i Cavity ring-down laser spectrometer, and δ^{13}C-CO_2 was analysed using thermo scientific MAT 253 isotope ratio mass spectrometer.

The average charge balance error for the analytical results is -0.1%. Data with charge balance error within the range of ±10% were used in further assessment while data out of this range were considered of low quality and not further considered. Therefore, data for 55 samples were used while data from nine samples were discarded.

3.2 Aqueous Speciation and Mineral Saturation Indices

The PHREEQC computer program and the llnl.dat database (Parkhurst and Appelo, 1999) were used to calculate the aqueous speciation, charge balance, activities, and activity coefficients of different aqueous species from component concentrations. It was also used to calculate the saturation indices (SI) which is used to assess the mineral-fluid equilibria, and is calculated by subtracting the logarithm of equilibrium constant (K) from the logarithm of reaction quotient (Q) for a particular reaction.

$$SI = \log Q - \log K \quad (1)$$

If SI<0 the water is undersaturated with respect to the mineral, which could thus be dissolving, if SI=0 the water is saturated, and if SI>0 the water is supersaturated and the mineral could be forming (precipitating). The saturation states of studied waters were assessed with

respect to albite, K-feldspar, K-mica, chalcedony, calcite, chlorite, alunite, kaolinite, gibbsite, hematite, goethite, quartz, talc, analcime, fluorite, illite, and chrysotile. These minerals have been identified in the area, while others are minerals commonly observed in the low temperature environments. To estimate the subsurface temperature, such mineral-fluid saturation was assumed using a multi-mineral equilibria geothermometry approach (Reed and Spycher, 1984). This technique involves calculation of the saturation index of relevant secondary minerals and solving the temperature where the mineral saturation indices are at equilibrium.

3.3 Relative Mobility of Elements

The relative mobility (RM) of elements in the surface waters and groundwater in the upper flanks of Mt. Meru volcano was calculated from the relationship,

$$RM = \left(\frac{Ci}{Na}\right)w \Big/ \left(\frac{Ci}{Na}\right)r \quad (2)$$

where Ci is the concentration of element *i* in water ´w´ and in rocks ´r´ in mmol/kg normalized to the concentration of sodium ´Na´. Sodium was selected as the reference element because it is abundant both in water and in the reference rock and it is the highly mobile cation (Gislason et al., 1996). The chemical composition of nephelinites, which were used as reference rocks due to their abundance in the area (BGR, 2018; Dawson, 2008; Roberts, 2002) is reported in Table 1**: Chemical composition of the nephelinites in the study area used for calculation of elemental relative mobility based on whole rock geochemistry. Data from (Roberts, 2002).** in the appendix. Elements with RM above the reference suggest they are controlled by dissolution of primary rocks while elements with low RM indicate they are retained in the host rocks or uptake by the secondary minerals.

4. RESULTS

4.1 Water Composition

The lake waters are the most saline in the study area with temperatures of 18.4-28.2 °C, pH of 7.1-9.9, EC of 1004-43600 µS/cm, and redox potential of -270 to 116 mV. The composition of major cations is dominated by Na (163-14350 ppm), K (89.4-1830 ppm), Ca (1.09-19 ppm), and Mg (2.18-9.31 ppm). Major anions are ΣCO_2 (556-13125 ppm), SO_4 (22.5-3186 ppm), Cl (29-1611 ppm), and F (2.77-1180 ppm). SiO_2 content for the lake waters is 2-52.2 ppm and isotopic composition of δ^2H-H_2O is -8.8 to 37 ‰, and $\delta^{18}O$-H_2O is -2.6 to 6.73 ‰. The saline-alkaline lakes indicate the highest concentration of Na, K, Mg, Al, Cl, F, SO_4, and ΣCO_2 among the studied waters (Figure 4-1). Groundwater had measured temperatures of 22-25 °C, pH of 6.5-8.6, EC of 257-786 µS/cm, redox potential of 59-238 mV, and SiO_2 (33.3-57.6 ppm). The determined concentration of major cations is dominated by Na (52.6-154 ppm), followed by K (13-33.9 ppm), Ca (2.86-5.49 ppm), and Mg (0.431-5.41 ppm). Major anion composition is dominated by ΣCO_2 (142-494 ppm), SO_4 (0.372-13.4 ppm), Cl (4.38-16.2 ppm), and F (4.24-15.7 ppm). The isotope composition was δ^2H-H_2O of -27.3 to -18.3 ‰, $\delta^{18}O$-H_2O of -5.67 to -3.97 ‰, and $\delta^{13}C$-CO_2 of -15.7 to -5.9 ‰.

Spring waters are characterized by discharge temperatures of 14.0-24.1 °C, pH of 6.3-8.9, EC of 242-9320 µS/cm, redox potential of -70 to 308 mV. The major elements composition in the springs is dominated by sodium (Na) (38.5-2294 ppm), followed by K (13.7-327 ppm), Ca (1.01-20.8 ppm), and Mg (0.351-6.78 ppm). Anions are dominated by, ΣCO_2 (98.1-3062 ppm), followed by SO_4 (2.07-1437 ppm), Cl (2.86-203 ppm), and F (1.43-77.9 ppm). The SiO_2 content is (4.4-72.1 ppm), isotopic composition of water is δ^2H-H_2O of -35.6 to -10.5 ‰ and $\delta^{18}O$-H_2O of -6.83 to -2.49 ‰ and for dissolved inorganic carbon is $\delta^{13}C$-CO_2 of -16.6 to -0.29 ‰. Among the springs, Njekukumia springs indicate the highest concentration of major elements (except for NO_3) compared to other springs and they occur as outliers in the box and whisker plots (Figure 4-1). Rivers and streams water have temperatures of 12.3-33.8 °C, pH of 6.3-9.6, EC of 109-5360 µS/cm, redox potential of 15-317 mV. The composition of major cations is dominated by Na (14.4-1211 ppm), K (7.5-207 ppm), Ca (1.42-18.7 ppm), and Mg (0.245-5.2 ppm). The concentration of major anions was dominated by ΣCO_2 (41.1-1801 ppm), SO_4 (0.124-564 ppm), Cl (1.45-167 ppm), and F (0.248-71.9 ppm). The SiO_2 content is (6.1-51 ppm), isotope composition for these waters is δ^2H-H_2O of -35.3 to -8.1 ‰, $\delta^{18}O$-H_2O of -6.81 to -2.25 ‰, and $\delta^{13}C$-CO_2 of -17.1 to 1.21 ‰.

The concentrations of trace alkali metals (Li, Rb, Cs) range between 0.005 ppb and 1179 ppb. Lithium concentrations are 0.4-105 ppb, Rb concentrations are 2-1179 ppb, and Cs concentrations are 0.005-0.725 ppb. The highest concentration of Li up to 94 ppb was detected in the springs. In the high pH saline-alkaline lakes, an elevated concentration of Li is observed reaching 64 ppb. The highest concentrations of Cs and Rb are 0.723 ppb and 1179 ppb, respectively, observed in the saline-alkaline lakes which have the highest pH among other waters. Significantly high concentrations of Rb reaching 291 ppb are observed in spring waters as well. The concentrations of trace alkaline earth metals (Be, Sr, Ba) are 0.008 ppb to 947 ppb. The concentrations of Be are 0.008-1.43 ppb, Sr concentrations are 25-947 ppb and Ba concentrations are 0.427-175 ppb. The highest concentration of Be, Sr and Ba (up to 1.43 ppb, 947 ppb and 175 ppb, respectively) are detected in springs while significantly high concentrations of Sr reaching up to 720 ppb are detected in the saline-alkaline lakes. The concentration of As, Cr, Ni, Pb, Se, Sn, Tl, V, and Zn range between 0.002 ppb and 3506 ppb. The concentrations of As are

0.046-32.8 ppb, of Cr are 0.4-16.2 ppb, Ni concentrations are 3.35-32.6 ppb, Pb concentrations are 0.146-1.31 ppb, concentrations of Se are 0.15-2.95 ppb, Sn concentration of 0.014-0.4 ppb, Tl concentrations of 0.002-0.07 ppb, V concentrations are 0.678-562 ppb, and concentrations of Zn are 0.479-3506 ppb. The highest values of concentrations of As, Cr, Ni, Pb, Se, Sn, Tl, V, and Zn were measured in the spring waters. Among the springs, Njekukumia springs are characterized by the highest concentrations of trace elements which occur as outliers compared to other springs.

The concentrations of B, Cd, Ga, Ge, Hf, Hg, Ho, In, Mo, Nb, Sb, Sc, Ta, Tb, Te, Th, Ti, U, W, Y, Zr range between 0.001 ppb and 2044 ppb. The concentrations of B are 3.73-2044 ppb, Cd are 0.003-1.1 ppb, Ga are 0.008-19 ppb, Ge are 0.001-0.385 ppb, Hf are 0.001-2.23 ppb, Hg are 0.003-3.95 ppb, Ho are 0.001-0.1 ppb, In are 0.001-0.008 ppb, Mo are 0.21-1558 ppb, Nb are 0.019-3.54 ppb. The concentrations of Sb are 0.017-0.8 ppb, Sc are 0.096-5.3 ppb, Ta are 0.001-0.652 ppb, Tb are 0.001-0.1 ppb, Te are 0.034-5 ppb, Th are 0.001-1 ppb, Ti are 0.6-240 ppb, U are 0.011-598 ppb, W concentrations are 0.093-971 ppb, Y are 0.021-3.01 ppb, Zr are 0.06-802 ppb. These elements indicated highest concentrations in the saline-alkaline lakes. The concentrations of Mn, Co, and Cu ranges between 0.04 ppb and 165 ppb. The concentration of Mn is 0.8-165 ppb, Co is 0.04-0.604 ppb, and Cu is 0.4-5.74 ppb. The elevated concentration of these metals was indicated in the rivers. The rare earth elements (REEs) including La, Ce, Pr, Nd, Sm, Eu, Gd, Tb, Dy, Ho, Er, Tm, Yb, and Lu indicated concentrations between 0.001 and 6.5 ppb. The concentrations of these elements are mostly below 1 ppb and values reaching 1 ppb were detected in a few samples. High concentration of La reaching 3.48 ppb is detected in the rivers, while in the saline-alkaline lakes concentration reaching 2 ppb was detected. Cerium is the most abundant REE with concentration reaching 6.5 ppb in river waters and 4.7 ppb in saline-alkaline lakes. The highest concentration of Nd (2.4 ppb) is detected in the alkaline lake waters while highest concentration of 2.27 ppb is observed in river waters. The Maji ya Chai River (TO-63) which has been identified to have the highest concentration of La, Ce, and Nd also exhibits high concentration of Cu and the highest concentration of Fe among the studied waters. Other REEs exhibit concentration magnitudes below 1 ppb. The studied waters were classified using the Piper plot (**Error! Reference source not found.**). This diagram indicates that both the springs-, lakes-, ground- streams and rivers water are dominated by $NaHCO_3$ composition.

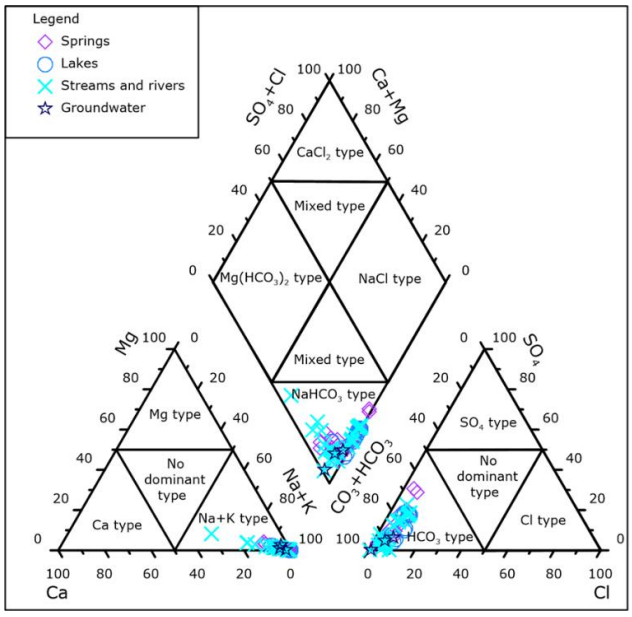

Figure 4-1: Piper plot showing the classification of the studied waters in the upper flanks of Mt. Meru volcano. The composition of surface and groundwaters is predominantly $NaHCO_3$.

5. DISCUSSION

5.1 Origin of Water

The majority of waters at Mt. Meru follow closely the water isotope ratio (δ^2H and $\delta^{18}O$) of the global meteoric water line (GMWL) and display similar values as the local precipitation, indicating a local meteoric water source of the surface and groundwaters (Figure 5- 1).

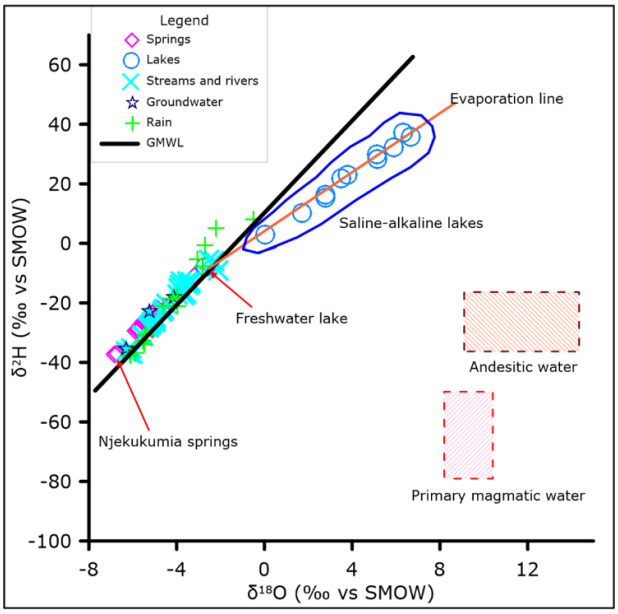

Figure 5- 1: Correlation plot of $\delta^{18}O$-H_2O vs $\delta^{2}H$-H_2O in per mil against standard mean ocean water (SMOW) for the studied waters in Meru. The GMWL is defined by the equation $\delta^{2}H = 8\delta^{18}O + 10$ (Craig, 1961). This plot suggests that the surface and groundwaters in Meru are of meteoric origin. End-member composition for andesitic and primary magmatic water are taken from Benavente et al. (2016) and Giggenbach (1992).

The streams, rivers, and freshwater lake plot along the GMWL trend whereas groundwaters are slightly shifted to lower $\delta^{18}O$ values similar to the local precipitation. The saline-alkaline lakes waters display higher $\delta^{2}H$ and $\delta^{18}O$ ratios compared to other water samples in the area. The lake samples follow a line with a slope of 4.91 corresponding to an enrichment resulting from free evaporation in the closed basin (Craig, 1961; Sharp, 2017).

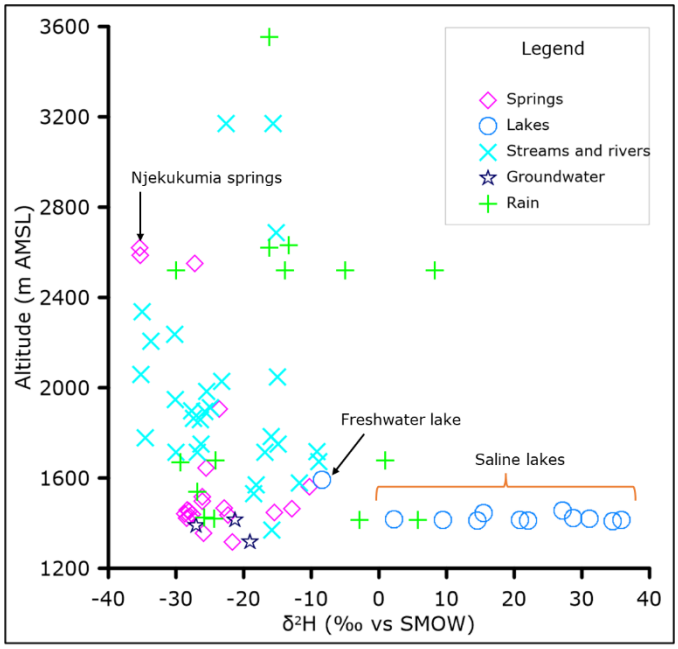

Figure 5- 2: Correlation plot of altitude and δ^2H-H_2O for different waters in the upper flanks of Mt. Meru volcano. This plot suggests that variability of δ^2H-H_2O at Mt. Meru is due to altitude effect and evaporation.

Moreover, the water samples show distinguished decrease in δ^2H with increasing altitude consistent with fractionation processes as a function of pressure and temperature (Sharp, 2017; White, 2020). Some rainwater samples indicate enrichment in δ^2H compared to springs, streams and rivers in the similar altitude suggesting they were evaporated prior to analysis (Figure 5- 2).

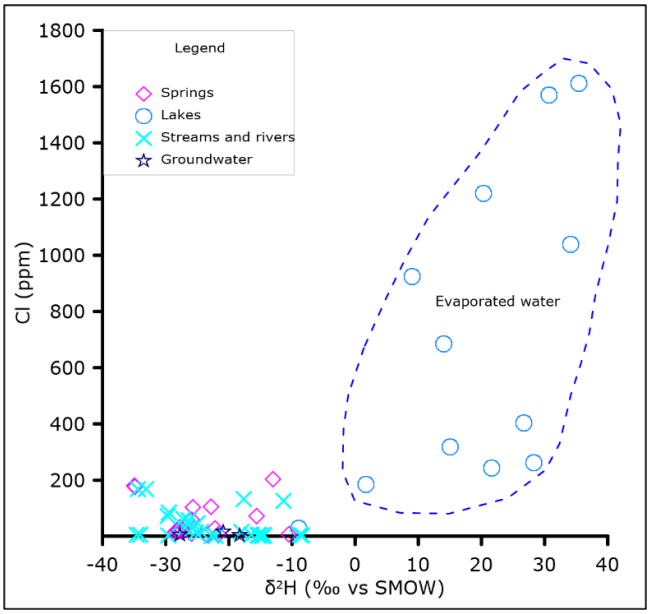

Figure 5- 3: Correlation plot of chloride and δ^2H-H_2O for the surface and groundwaters in the upper flanks of Mt. Meru volcano.

The shift in water isotopes in the saline-alkaline lakes of Mt. Meru is consistent with high concentration of dissolved constituents in these lakes. Similar enrichment has been observed in the Olkaria Domes and Olkaria East high temperature geothermal reservoir fluid and in the Nakuru and Elementaita rift lakes in Kenya (Mutonga, 2015). The chloride vs δ^2H-H_2O plot suggest that most waters at Mt. Meru show low Cl concentrations and the δ^2H isotope ratios are controlled by precipitation altitude. The saline-alkaline lake waters are enriched in all major elements with somewhat irregular δ^2H isotope ratios presumably caused by open system evaporation and condensation processes (Figure 5- 3). No obvious signs of thermal water inputs are observed, for example decreasing Mg content and increasing SiO_2 concentration with δ^2H water ratios of the saline-alkaline lake waters.

5.2 Relative Mobility of Elements

The relative mobility (RM) of a particular element can be used to gain insight into its behavior upon water-rock interaction. Assuming Na (i.e., the reference element) to be mobile, lower RM suggests uptake of the element into secondary minerals. Almost all elements show lower mobility compared to Na (Figure 5-4).

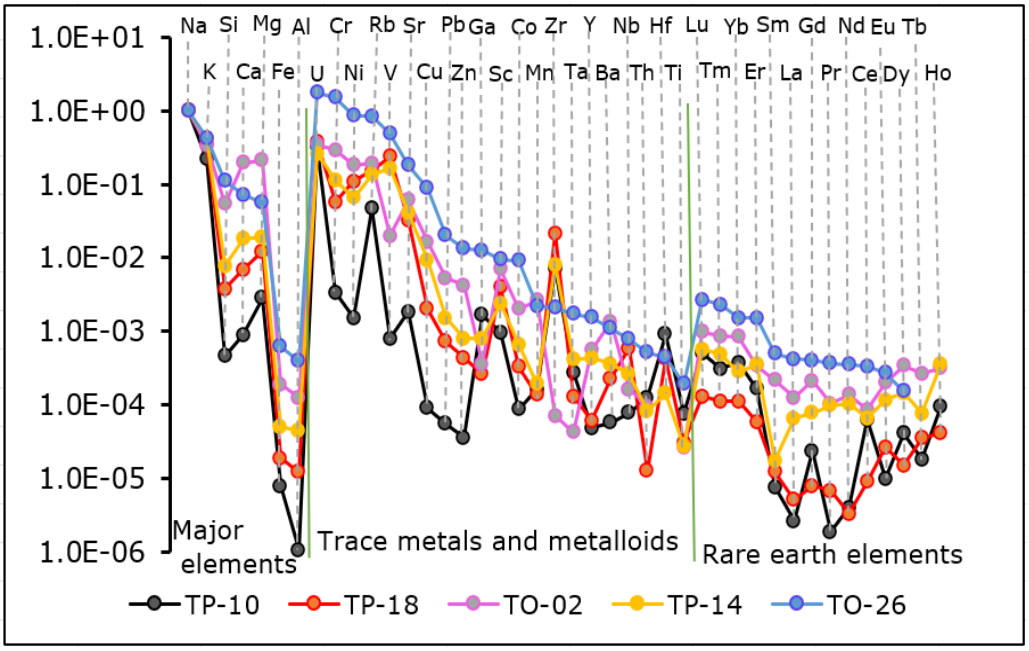

Figure 5- 4: Relative mobility of major-, trace-, and rare earth elements in different water types in the Mt. Meru volcano area. TP-18 is the Njekukumia spring, TP-02 is a dilute cold spring. TP-14 is Ngarenayuki river, TP-10 is the saline-alkaline Big Momella lake, and TO-26 is groundwater.

Among major elements, Na and K are the most mobile whereas Al and Fe are the least mobile. Other major elements (Si, Ca, and Mg) also show reduced mobility relative to Na suggesting majority of these elements are retained within alteration minerals upon water-rock interaction. The low mobility of Al and Fe suggest they are completely retained into alteration and weathering minerals like aluminium silicates and/or oxides and hydroxides. Trace elements show a similar span in RM values as major elements. In all waters, U, Cr, Ni, Rb, V, Sr and Cu show the highest mobility while Th and Ti are the least mobile among trace elements. The elements with high mobility are probably controlled by dissolution of primary rocks while elements with low mobility are likely incorporated in the secondary minerals. The relatively high aqueous mobility of some trace elements is consistent with the aqueous speciation distribution predominated by simple ions (Rb^{+}, Sr^{+2}, and Ni^{+2}) or formation of highly soluble oxyanion complexes in water (U). In other cases, the RM of some elements is unknown due to lack of data on trace element composition of rocks in the study area.

The Rare Earth Elements (REE) have similar chemical properties and generally display low solubilities, however they can be mobilized and fractionated during surface alteration of rocks (Wayne Nesbitt, 1979). The REE generally show low relative mobility in the surface and groundwaters (Figure 5- 4) suggesting they are mostly retained in the host rocks and incorporated into alteration and weathering minerals. This behaviour was also observed in the weathering profile by Middelburg et al. (1988). The aqueous mobility of the REE gradually increases with increasing atomic number thus the heavy rare earth elements (HREE) are slightly mobile compared to the light rare earth elements (LREE) suggesting increasing solubility. The increase in solubility with increasing atomic number is consistent with preferential leaching of HREE from host rocks compared to LREE (Wayne Nesbitt 1979) while LREE are preferentially enriched in the rock residue (Braun et al., 1993). The variability in the magnitude and pattern of RM in different waters can be attributed to different and complex processes such as incongruent dissolution of these elements from the host rocks, redox processes, uptake by secondary minerals, ion exchange between minerals, and transport reactions (Aiuppa et al., 2005, 2006; Middelburg et al., 1988). It may also indicate that these waters interact with different rocks, not only nephelinites as assumed in this study but also other rock types for example phonolites, tephriphonolite, phonotephrite which were also identified at Mt. Meru (Roberts, 2002).

5.3 Aqueous Speciation and Mineral Saturation Indices

The geochemical behavior of elements including reactivity and precipitation into alteration and weathering minerals largely depends on their aqueous speciation. The speciation calculation indicates ligands in the studied waters are Cl as Cl^{-}, CO_2 as HCO_3^{-} and CO_3^{2-}, F as F^{-}, Br as Br^{-}, N as NO_3^{-}, and S as SO_4^{2-}. Speciation results indicate that the most important ligands in the waters of the upper flanks of Mt. Meru volcano are dissolved carbon (HCO_3^{-} and CO_3^{2-}), fluoride (F^{-}), and water (OH^{-}). The abundance of complexes formed between the

metals and chloride (Cl^-) and sulfate (SO_4^{2-}) is low compared to other ligands. The number of complexes formed between these ligands and different metals can be associated with the reactivity/affinity of these metals with such ligands.

Knowing the aqueous species concentrations, the relevant mineral saturation indices can be estimated (Figure 5-5). Various secondary minerals including ferric oxide, alunite, gibbsite, kaolinite, levynite, K-feldspars, hematite, smectite, halloysite, carbonates, and native sulfur have been identified at Mt. Meru (Lyu et al., 2018; Mahecha, 2019). Among the identified minerals, some are typical argillic alteration minerals (acid sulfate alteration) like ferric oxide, alunite, gibbsite, kaolinite, hematite, and native sulfur whereas others, for example halloysite are low temperature weathering minerals while K-feldspar can be observed in both low and high temperature conditions as well as in igneous rocks. Alunite ($KAl_3(SO_4)_2(OH)_6$) is undersaturated in the studied waters suggesting that it is unstable. In fact, its occurrence can be related to argillic alteration rather than weathering and low temperature alteration. The minerals analcime, hematite, K-feldspar, and goethite are, in contrast, supersaturated and may form.

The saturation index of kaolinite, alunite, gibbsite, analcime, and K-feldspar, and quartz decreases with increasing pH with significant decreases at pH above 8. This is because of the dissociation of aqueous silicic acid to form $H_3SiO_4^-$ at pH > 8 therefore the activity of H_4SiO_4 decreases hence log Q value for species that include the H_4SiO_4 (Brady and Walther, 1989; White, 2020). The saturation indices of other minerals, calcite, fluorite, and Mg-silicates (chrysotile and talc) increase with increasing pH while hematite and goethite seem to be pH independent in the range of the studied waters. The supersaturation of water with Al and Fe secondary minerals is consistent with the low RM indicated by Al and Fe (Figure 5- 4). Trace elements indicated to have low RM could be substituting for major elements in the forming secondary minerals (**Error! Reference source not found.**). For example, Mn, Ni and Co could be substituting for Fe while the trivalent metals like Sc could be substituting for Al. The elements Ba and Sr are known to be incorporated in the Al-silicates (Kaasalainen and Stefánsson, 2012) and references therein. Formation of low temperature weathering minerals at Mt. Meru could be enhanced by humid and temperate climate (Lyu et al., 2018).

5.4 Water-Rock Interaction and Mixing

In general, the process of water-rock interaction influencing water composition at Mt. Meru may be described by an incongruent weathering of nephelinites. Such would imply primary minerals and glasses to be dissolved to variable degree and other weathering minerals formed that have different relative elemental composition to the primary minerals. The wide variability in the composition of the studied waters may be due to difference in the specific lithology interacting with water, varying degree of dissolution, difference in residence time, and admixture of volatiles of deep provenance in some of these waters. The waters at high altitude (except the Njekukumia springs) are dilute indicating they are less reacted. Enrichment of dissolved constituents increases with decreasing altitude indicating water-rock reaction time is an important factor controlling water composition thus waters at low altitude are more reacted.

The composition of the studied waters suggest to be controlled by chemical weathering (dissolution of rocks at low temperature) without significant input of geothermal water. The positive correlation between major constituents like Na, K, Mg, SO_4 and the conservative Cl (Figure 5- 5) and trace elements vs Cl (Figure 5- 7) suggest progressive water rock interaction at low temperature and mixing of variable reacted non-thermal waters as the dominant processes controlling water composition. The increase of Mg concentration with increasing Cl is indicative of low temperature water-rock interactions (weathering) and that with more rocks being dissolved the more Mg gets into the water. The concentration of SiO_2 in the studied waters is low indicative of typical continental rock weathering. The lack of linear trend on the SiO_2 vs Cl plot suggests insignificant input of geothermal fluid. Furthermore, the positive correlation of ΣCO_2 and Cl suggest the CO_2 to originate mainly from dissolution carbonates, possibly trona identified in the area.

The dissolution of rocks may be enhanced by admixture of volcanic gases in some springs indicated by relatively high concentration of rock forming elements than in other springs. During chemical weathering CO_2 is converted to HCO_3 leading to increased concentration of HCO_3 with increasing concentration of dissolved rock forming elements which is considered as the index of water-rock-gas interaction (Aiuppa et al., 2000, 2005). Equation (3) indicates an example of CO_2 consuming reaction during chemical weathering of rocks.

$$CaAl_2Si_2O_8 + 2CO_2 + 3H_2O = Al_2Si_2O_5(OH)_4 + 2HCO_3^- + Ca^{2+} \quad (3)$$

Anorthite kaolinite

In addition to the interaction of water with alkali volcanic rocks, composition may also be influenced by the dissolution of evaporites that form on the surface during the dry season due to enhanced evaporation and get flushed at the onset of rainy season (Malago et al., 2020; Nanyaro et al., 1984).

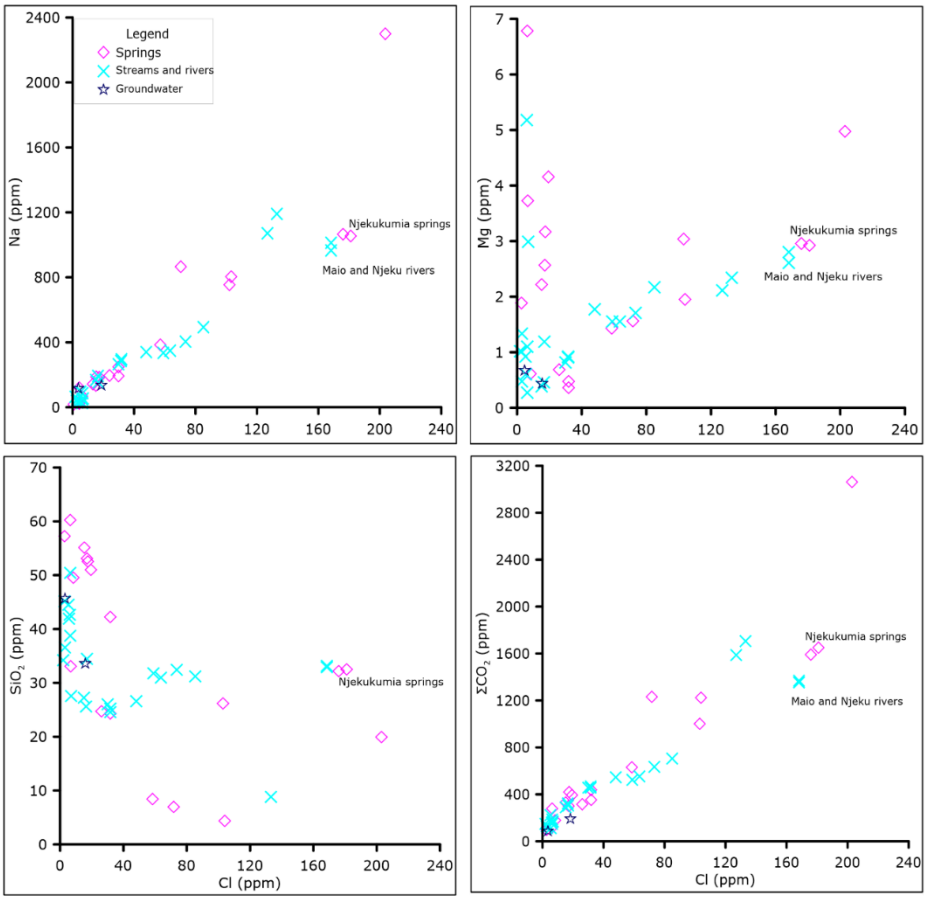

Figure 5- 5: Correlation plot of Cl and Na, Mg, SiO_2 and ΣCO_2 in the surface and groundwater on the upper flanks of Mt. Meru volcano. These plots suggest that the composition of the spring-, stream-, river-, and groundwater is mainly controlled by weathering of rocks at low temperature.

The composition of the waters at Mt. Meru is also affected by the mixing of waters from different sources. There are possible two end-member water compositions in the study area, which are dilute waters (non-reacted or waters with low residence time) and more reacted waters. The non-reacted water has low concentration of dissolved constituents, while the reacted is somewhat mineralized. The reacted waters are indicated by for example the Njekukumia springs and few other springs (Figure 5- 7) whereas other springs, rivers, streams, and groundwater indicate varying degrees of mixing with non-reacted water. The reacted water end-member may be enhanced by dissolution of rocks by action of CO_2 charged water as a result of input of CO_2 from deep sources (Ghiglieri et al., 2012; Grassa et al., 2006). The hydrological flow map indicates how the springs, streams and rivers join and mix in the study area (Figure 5- 6). The Maio and Njeku rivers are the highest mineralized among streams and rivers (Table 2) suggesting they mix with reacted waters possibly from springs (Figure 5- 7 and Figure 5- 8). Upon mixing, the mobile elements like Cl, B, As, and Li (Aiuppa et al., 2005, 2006; Kaasalainen and Stefánsson, 2012), indicate linear trends (Aiuppa et al., 2006; Arnórsson, 1985; Kaasalainen and Stefánsson, 2012). The elements Na, K, F, and SO_4 are also mobile upon mixing (Figure 5- 7) while others including SiO_2, Fe, Al, Ca, W, Sb, Sr, V, U, W, Zr do not show linear trend with chloride suggesting they react upon mixing.

Along the river flow path, the increasing dilution/mixing is evident. Two samples were collected in the Ngarenanyuki river, TP-14 was collected upstream close to the mini-hydropower plant in the Arusha National Park (ANP) while TP-65 was collected downstream close to the ANP headquarters. Analysis of the two samples indicate a systematic decrease in the physicochemical parameters and major elements in a 2.5 km river flow path. EC, Na, K, Ca, Mg, Fe, F, Cl, ΣCO_2, and SO_4 decreased by different order of magnitudes between 20 % and 40 %. However, there was no river identified to join Ngarenanyuki river between the two sampling points (Figure 5- 6), although there may be small streams or underground sources not detected by remote sensing (SRTM) which may be causing dilution. Considering

the significant change in the chemical composition of Ngarenanyuki river in such a short flow path (2.5 km), it indicates that geochemical processes operate at relatively high rate in the surface conditions.

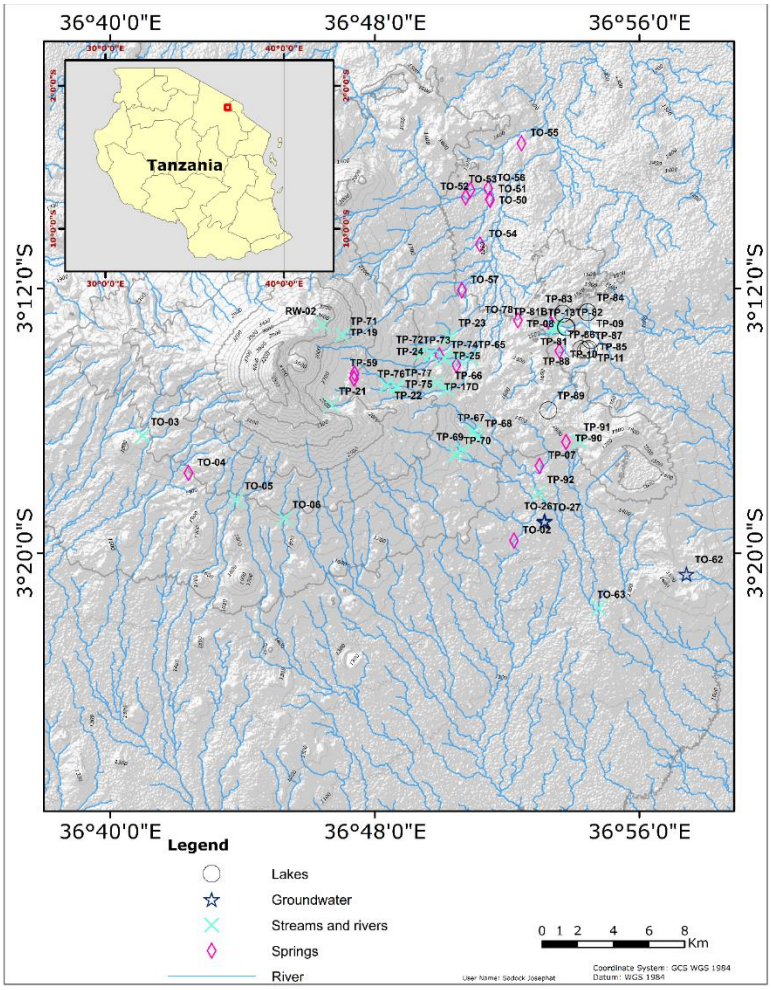

Figure 5- 6: Map showing hydrology in the Mt. Meru area. Sampling sites for this study and sample numbers are also indicated.

Nasula river is characterized by high concentration of some trace elements (Figure 5- 7 and **Error! Reference source not found.**). The highest concentration of B (667 ppb), Li (105 ppb), Sb (0.362 ppb), Sr (941 ppb), As (31.7 ppb), and W (125 ppb) were identified in this river compared to other studied waters. However, this river evinces low concentration of major elements. This river is located on the lower altitude, 1670 m AMSL compared to the Njekukumia springs 2615 m AMSL on the eastern flank of Mt. Meru volcano. The low concentration of major elements and high concentration of trace elements may be associated with non-congruent dissolution of host rocks and a range in geochemical behaviors between the major and trace elements.

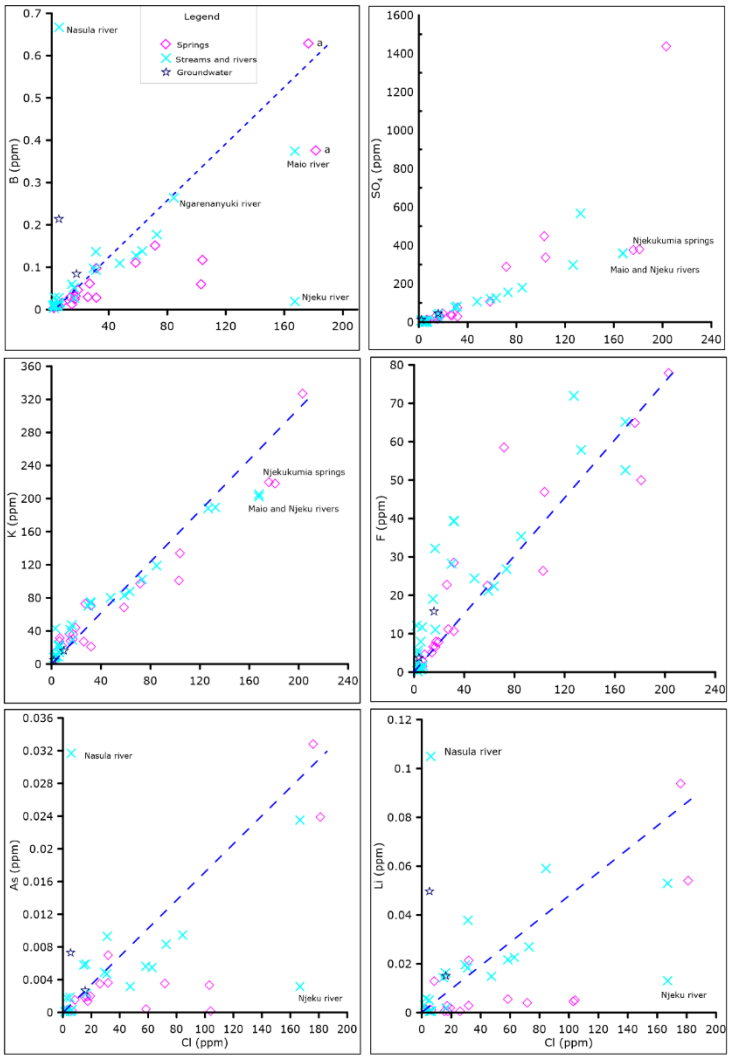

Figure 5- 7: Correlation plots for chloride and boron, sulfate, potassium, fluoride, arsenic, and lithium in the spring-, stream-, river- and groundwaters. The letter 'a' represents Njekukumia springs.

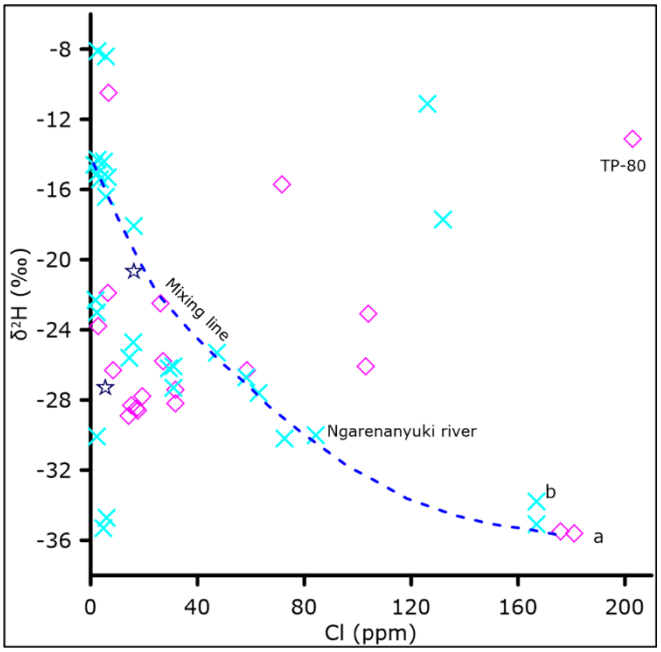

Figure 5- 8: Correlation plot of δ^2H-H_2O and chloride for the spring-, stream-, river-, and groundwaters in the upper flank of Mt. Meru volcano. The letters 'a' represent Njekukumia springs while 'b' represent the Maio and Njeku rivers.

Based on the composition of the studied waters, two end-member water compositions are inferred at Mt. Meru. These include the dilute (nearly fresh rainwater) and the reacted waters (possibly with some input of deep gases). Other waters are the results of mixing between the two endmembers.

5.5 Carbon Source in the Water at Meru

The studied waters are enriched in CO_2 similar to many other areas in the East African Rift System. Dissolved carbon concentrations show positive correlation with many other elements, for example Na, K, Mg, and Ca suggesting the source of CO_2 to be progressive water-rock interaction with carbon rich rocks. Alternatively, magmatic degassing through Mt. Meru volcano is another possibility for the sources of CO_2. The δ^{13}C-CO_2 data support such a hypothesis, with mixing of CO_2 of deep origin characterized by CO_2 with δ^{13}C similar to mantle gas, surface CO_2 of atmospheric and biogenic origin (Figure 5- 9) (Chiodini et al., 2008; Delalande et al., 2011; Grassa et al., 2006).

Carbon dioxide is among the least soluble volatile in melts at high pressure resulting in degassing potentials from deep levels through the crust to surface without any magma transfer or deep geothermal activity (e.g., Ranta et al., 2023). Also, the input of deep provenance volatiles into the Njekukumia springs is supported by the presence of acid-sulfur alteration mineralogy in the vent of ash cone ~2 km west of these springs. Fumarolic activities were also observed at the ash cone vent until 1954 (Ghiglieri et al., 2010; Wilkinson et al., 1986). However, recent attempt to map such activity in June 2017 using thermal imaging camera could not identify a thermal anomaly in the area. There have also been field observations in October 2016, June 2017, July 2018, and June 2021 but no fumarolic activity have been identified. The Lendoiya springs at low altitude also suggest input of deep CO_2. It is likely that the flux of volatiles from deep provenance has been largely quenched by cold water flowing from the high altitudes of Mt. Meru volcano, regarded as the recharge zone. The volatiles from deep sources may be carried with groundwater water along the flow path. It is also possible that hydrothermal degassing may have decreased due to recession of the water table.

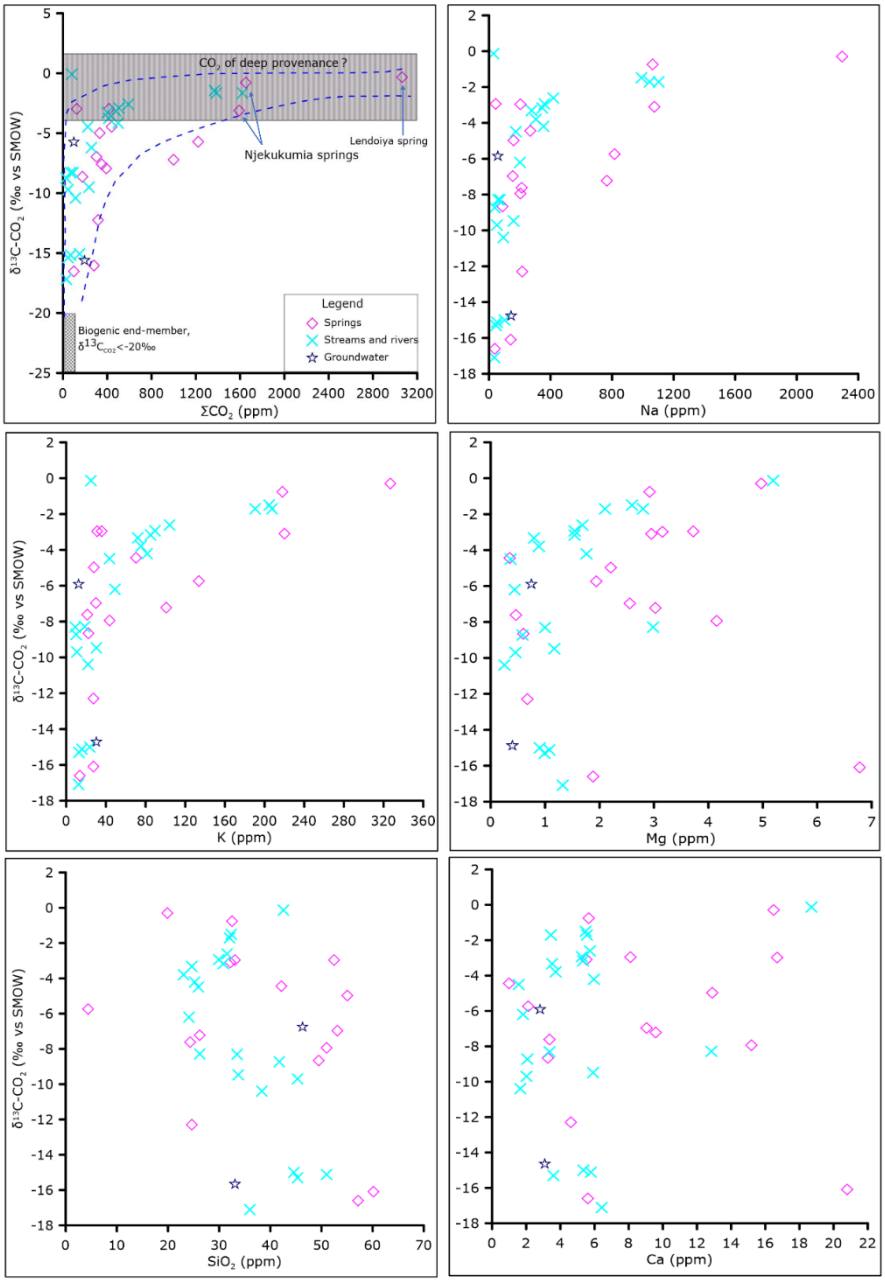

Figure 5- 9: Correlation plot of $\delta^{13}C\text{-}CO_2$ and ΣCO_2, Na, K, Mg, SiO_2 and Ca for the springs-, streams-, rivers-, and groundwater while $\delta^{13}C\text{-}CO_2$ was not analyzed in the lake samples. The end-member composition for $\delta^{13}C\text{-}CO_2$ is from Chiodini et al. (2008) and Grassa et al. (2006).

5.6 Geothermal Fluids at Mt. Meru

The reacted water at high altitude indicated by the Njekukumia springs, discharge waters with a little elevated temperature (23 °C) compared to nearby springs and local ambient temperature (12 °C). Such is in line with previous studies at Mt. Meru (Bennett, 2022; Bennett et al., 2021; Ghiglieri et al., 2012) suggest the occurrence of thermal waters. The thermal water may be a result of shallow circulation of meteoric water and heat mining from the cooling rocks while input of deep gas to these springs is suggested based on $\delta^{13}C\text{-}CO_2$. To characterize the potential temperatures of such thermal waters, the multi-mineral equilibria geothermometry approach (Reed and

Spycher, 1984) was applied. Minerals which are commonly observed in low temperature systems including chalcedony, illite, K-feldspar, chlorite, fluorite, albite, and calcite were used. The results (Figure 5- 10) indicate potentially somewhat higher temperatures than observed at surface, i.e. between ~50 and 100 °C. Previous reservoir temperature estimation at Mt. Meru using quartz geothermometer suggested a temperature of 50 - 90 °C (Bennett, 2022). Moreover, the two springs (Figure 5- 10) indicate a similar range of reservoir temperature and identical chemical composition suggesting they originate from the same source. However, the temperature indicated by these springs may be non-relevant since water in these springs may represent a complex mixture of non-thermal waters of different origin (reacted and dilute cold waters) and potential thermal water as well. The results point towards a possible low-temperature thermal water (<100 °C) on the eastern flank of Mt. Meru but signs of intensive geothermal activity and a high-temperature geothermal system are lacking.

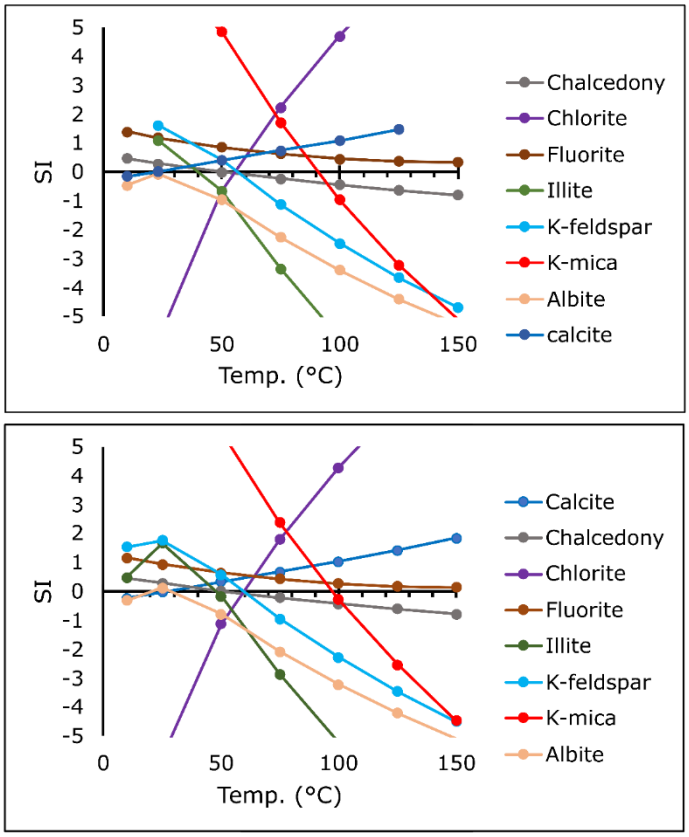

Figure 5- 10: Temperature versus saturation index plots for the Njekukumia springs, sample TP-18 (top) and TP-58 (bottom).

5.8 **Hydrogeology of Mt. Meru**

The hydrogeology and geochemistry of the natural waters at Mt. Meru reflects various elemental sources, progressive water-rock interaction and mixing of various water components. The waters are of meteoric origin, and infiltrate through permeable formations and fractures at high altitude and flow downslope at surface but mainly as subsurface groundwater. Along the flow-path the groundwaters continue to react with the surrounding rocks and minerals resulting in increased concentrations of dissolved constituents (Figure 5- 11). At relatively high altitude, waters of the Njekukumia springs display high dissolved element concentration relative to the surrounding spring waters, suggesting a possible input of more reacted and/or thermal water. The Njekukumia springs may therefore represent a relatively shallow circulation of meteoric water gaining temperature by conduction from rocks and mixing with gases of deep provenance (Figure 5- 12). According to a mixing model, Maio, and Ngarenanyuki rivers incorporate significant amount of water from the presumably Njekukumia thermal springs.

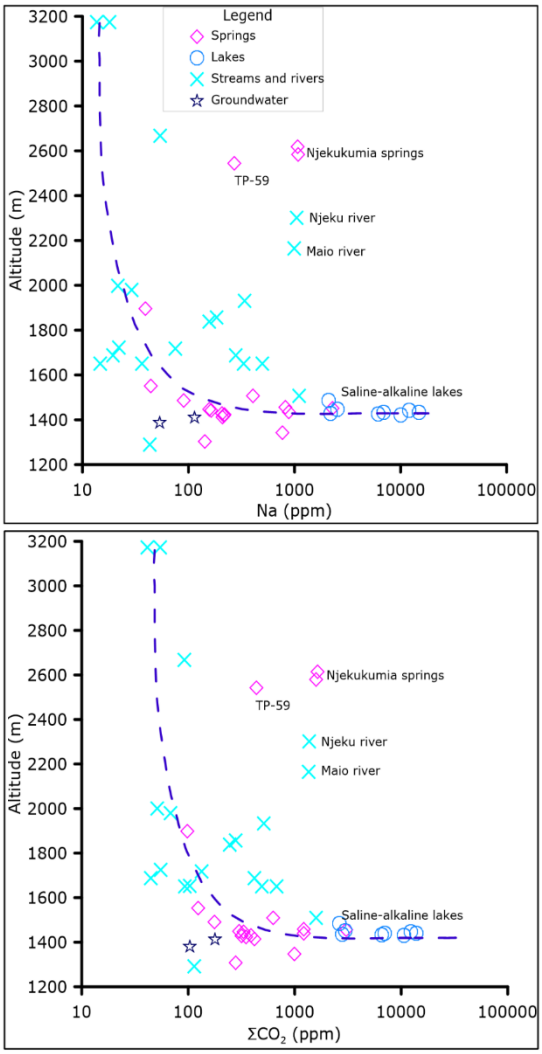

Figure 5- 11: Correlation plots for altitude and most abundant cation and anion in the studied waters. The hypothesized water chemistry evolution path is indicated by a blue dotted line. The Njekukumia springs with reacted water and Njeku and Maio rivers mixing with reacted waters evince high mineralization in the high altitude. The Lendoiya spring overlaps with saline - alkaline lakes.

The hydrological flow at Mt. Meru is hypothesized to be relatively fast due to the steep geomorphology of the area where the studied waters occur in the altitude between 1230 and 3554 m AMSL and the summit is 4565 m AMSL. No hydrological connection was identified on the surface between the saline-alkaline lakes and the Njekukumia springs and major rivers. The waters in saline-alkaline lakes are of meteoric origin as well but have been modified by the open system evaporation as indicated by enrichment in heavy stable water isotopes ($\delta^{2}H$ and $\delta^{18}O$) and dissolved elements, both major and trace elements. No clear signs of thermal water input in these lakes were identified in this study. There was no major surface inflow to these lakes observed in the field nor mapped by remote sensing.

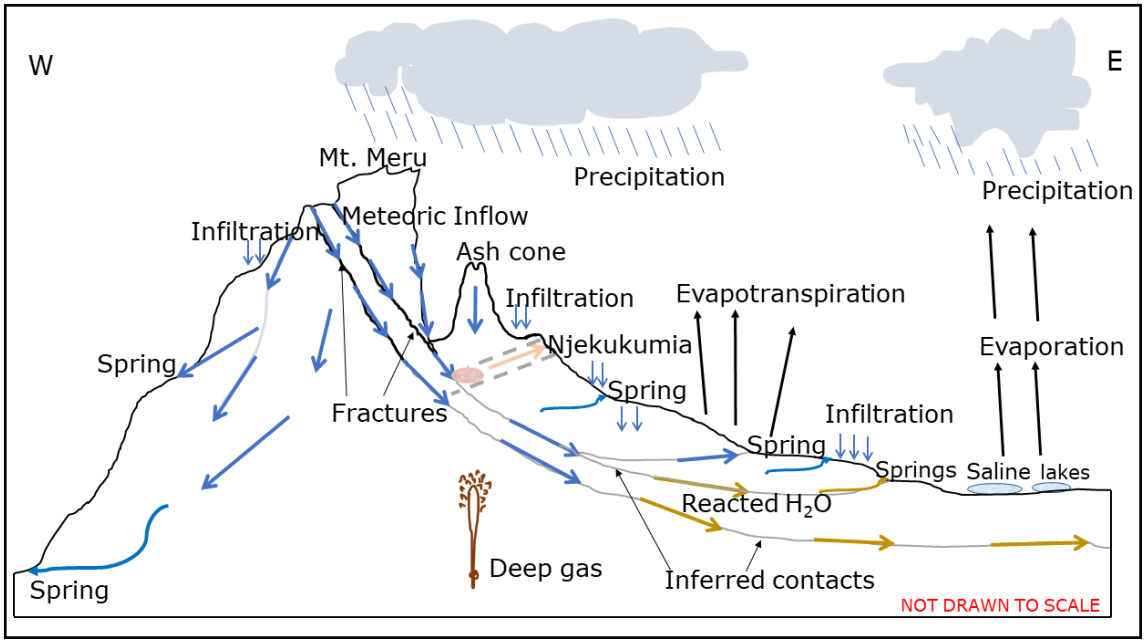

Figure 5- 12: Hypothesized waterflow model of the Mt. Meru volcano. Water infiltrates through the fractures/faults observed in the summit area and the crater at the top of ash cone. In the subsurface water could be flowing in the fractures or along lithological contacts.

6. CONCLUSION

The investigated waters are of meteoric origin as indicated by the stable water isotopes (δ^2H-H_2O and δ^{18}O-H_2O), with Na-HCO_3 composition. Their isotopic and chemical composition is affected by isotopic fractionation with altitude, evaporation, and condensation processes. The water precipitated at high altitude flows downslope partly at surface but mainly as subsurface groundwater. The correlation between major constituents (Na, K, Mg, SO_4, and Cl) suggests progressive water rock interaction at low temperature as the dominant process controlling water composition. No significant input of geothermal water was identified. The saline alkaline lakes appear to be formed by evaporative concentration of waters sourced at higher altitude. Two possible end-member water compositions, non-reacted and more reacted, have been identified, with other spring-, river- and groundwaters falling between these two end members, suggesting mixing. The δ^{13}C-CO_2 data suggest that main sources of dissolved inorganic carbon are dissolution of carbonates, mixing with biogenic CO_2 and input of deep volatiles.

Relative mobility of elements is generally low, only U and Cr have higher mobility than Na in the groundwater. Of the major elements, Na and K are the most mobile whereas other major cations show low mobility, suggesting that they are retained in alteration minerals upon water-rock interaction. Among trace elements U, Cr, Ni, Rb, V, Sr and Cu show the highest mobility, but Th and Ti are the least mobile, suggesting that the former are controlled by dissolution of primary rocks whereas the latter are incorporated into secondary minerals. The multi-mineral equilibria geothermometer suggests an equilibrium temperature of 50-100 °C for the Njekukumia springs. No signs of intense geothermal activity or a high-temperature geothermal system are observed.

ACKNOWLEDGEMENT

This paper is based on the Masters' thesis completed by the main author at the University of Iceland in 2023. I would like to thank GRÓ.GTP under the auspices of UNESCO for financially supporting my MSc studies and this research at the University of Iceland. I also thank my current employer Tanzania Geothermal Development Company Ltd (TGDC) for granting me permission to use the water chemistry data of the Mt. Meru area for this study.

REFERENCES

Aiuppa, A., Allard, P., D'Alessandro, W., Michel, A., Parello, F., Treuil, M., & Valenza, M. (2000). Mobility and fluxes of major, minor and trace metals during basalt weathering and groundwater transport at Mt. Etna volcano (Sicily). *Geochimica et Cosmochimica Acta*, *64*(11), 1827–1841. https://doi.org/10.1016/S0016-7037(00)00345-8

Aiuppa, A., Avino, R., Brusca, L., Caliro, S., Chiodini, G., D'Alessandro, W., Favara, R., Federico, C., Ginevra, W., Inguaggiato, S., Longo, M., Pecoraino, G., & Valenza, M. (2006). Mineral control of arsenic content in thermal waters from volcano-hosted hydrothermal systems: Insights from island of Ischia and Phlegrean Fields (Campanian Volcanic Province, Italy). *Chemical Geology*, *229*(4), 313–330. https://doi.org/10.1016/j.chemgeo.2005.11.004

Aiuppa, A., Federico, C., Allard, P., Gurrieri, S., & Valenza, M. (2005). Trace metal modeling of groundwater–gas–rock interactions in a volcanic aquifer: Mount Vesuvius, Southern Italy. *Chemical Geology*, *216*(3), 289–311. https://doi.org/10.1016/j.chemgeo.2004.11.017

Allegre, C. J. (2008). *Isotope geology*. Cambridge University Press.

Arnórsson, S. (1985). The use of mixing models and chemical geothermometers for estimating underground temperatures in geothermal systems. *Journal of Volcanology and Geothermal Research*, *23*(3), 299–335. https://doi.org/10.1016/0377-0273(85)90039-3

Arnórsson, S., & Andrésdóttir, A. (1995). Processes controlling the distribution of boron and chlorine in natural waters in Iceland. *Geochimica et Cosmochimica Acta*, *59*(20), 4125–4146. https://doi.org/10.1016/0016-7037(95)00278-8

Benavente, O., Tassi, F., Reich, M., Aguilera, F., Capecchiacci, F., Gutiérrez, F., Vaselli, O., & Rizzo, A. (2016). Chemical and isotopic features of cold and thermal fluids discharged in the Southern Volcanic Zone between 32.5°S and 36°S: Insights into the physical and chemical processes controlling fluid geochemistry in geothermal systems of Central Chile. *Chemical Geology*, *420*, 97–113. https://doi.org/10.1016/j.chemgeo.2015.11.010

Bennett, G. (2022). *Hydrogeological investigation of a volcanic aquifer system on the flanks of mount Meru, Northern Tanzania* [PhD Thesis]. Ghent University.

Bennett, G., Reybrouck, J., Shemsanga, C., Kisaka, M., Tomašek, I., Fontijn, K., Kervyn, M., & Walraevens, K. (2022). Identification of low fluoride areas using conceptual groundwater flow model and hydrogeochemical system analysis in the aquifer system on the flanks of an active volcano: Mount Meru, Northern Tanzania. *Science of The Total Environment*, *814*, 152682. https://doi.org/10.1016/j.scitotenv.2021.152682

Bennett, G., Van Reybrouck, J., Shemsanga, C., Kisaka, M., Tomašek, I., Fontijn, K., Kervyn, M., & Walraevens, K. (2021). Hydrochemical Characterisation of High-Fluoride Groundwater and Development of a Conceptual Groundwater Flow Model Using

Combined Hydrogeological and Hydrochemical Approach on an Active Volcano: Mount Meru, Northern Tanzania. *Water*, *13*(16), Article 16. https://doi.org/10.3390/w13162159

BGR. (2018). *Petrography of Rocks collected during the geothermal Field Visit of Mt. Meru, in October 2016* (p. 109) [Unpublished TGDC Report].

Brady, P. V., & Walther, J. V. (1989). Controls on silicate dissolution rates in neutral and basic pH solutions at 25°C. *Geochimica et Cosmochimica Acta*, *53*(11), 2823–2830. https://doi.org/10.1016/0016-7037(89)90160-9

Braun, J.-J., Pagel, M., Herbilln, A., & Rosin, C. (1993). Mobilization and redistribution of REEs and thorium in a syenitic lateritic profile: A mass balance study. *Geochimica et Cosmochimica Acta*, *57*, 4419–4434. https://doi.org/10.1016/0016-7037(93)90492-F

Chiodini, G., Caliro, S., Cardellini, C., Avino, R., Granieri, D., & Schmidt, A. (2008). Carbon isotopic composition of soil CO2 efflux, a powerful method to discriminate different sources feeding soil CO2 degassing in volcanic-hydrothermal areas. *Earth and Planetary Science Letters*, *274*(3), 372–379. https://doi.org/10.1016/j.epsl.2008.07.051

Chorowicz, J. (2005). The East African Rift System. *Journal of African Earth Sciences*, *43*, 379–410.

Craig, H. (1961). Isotopic Variations in Meteoric Waters. *Science*, *133*(3465), 1702–1703. https://doi.org/10.1126/science.133.3465.1702

Dawson, J. B. (1992). Neogene tectonics and volcanicity in the North Tanzania sector of the Gregory Rift Valley: Contrasts with the Kenya sector. *Tectonophysics*, *204*(1), 81–92. https://doi.org/10.1016/0040-1951(92)90271-7

Dawson, J. B. (2008). *The Gregory Rift Valley and Neogene—Recent Volcanoes of Northern Tanzania*. https://doi.org/10.1144/M33

Delalande, M., Bergonzini, L., Gherardi, F., Guidi, M., Andre, L., Abdallah, I., & Williamson, D. (2011). Fluid geochemistry of natural manifestations from the Southern Poroto–Rungwe hydrothermal system (Tanzania): Preliminary conceptual model. *Journal of Volcanology and Geothermal Research*, *199*(1), 127–141. https://doi.org/10.1016/j.jvolgeores.2010.11.002

Delcamp, A., Kwelwa, S., Macheyeki, A., & Kervyn, M. (2013). *Multiple collapses at Mt Meru volcano, Tanzania: Remote sensing and field evidences from debris avalanche deposits*. 7775.

Delcamp, A., Roberti, G., & van Wyk de Vries, B. (2016). Water in volcanoes: Evolution, storage and rapid release during landslides. *Bulletin of Volcanology*, *78*. https://doi.org/10.1007/s00445-016-1082-8

Didas, M. M., Armadillo, E., Hersir, G. P., Cumming, W., & Rizzello, D. (2022). Regional thermal anomalies derived from magnetic spectral analysis and 3D gravity inversion: Implications for potential geothermal sites in Tanzania. *Geothermics*, *103*, 102431. https://doi.org/10.1016/j.geothermics.2022.102431

Foster, A. N., Ebinger, C., Mbede, E., & REX, D. (1997). Tectonic development of the northern Tanzania sector of the East African Rift System. *Journal of The Geological Society - J GEOL SOC*, *154*, 689–700. https://doi.org/10.1144/gsjgs.154.4.0689

Ghiglieri, G., Balia, R., Oggiano, G., & Pittalis, D. (2010). Prospecting for safe (low fluoride) groundwater in the Eastern African Rift: The Arumeru District (Northern Tanzania). *Hydrology and Earth System Sciences*, *14*(6), 1081–1091. https://doi.org/10.5194/hess-14-1081-2010

Ghiglieri, G., Pittalis, D., Cerri, G., & Oggiano, G. (2012). Hydrogeology and hydrogeochemistry of an alkaline volcanic area: The NE Mt. Meru slope (East African Rift – Northern Tanzania). *Hydrology and Earth System Sciences*, *16*(2), 529–541. https://doi.org/10.5194/hess-16-529-2012

Giggenbach, W. F. (1992). Isotopic shifts in waters from geothermal and volcanic systems along convergent plate boundaries and their origin. *Earth and Planetary Science Letters*, *113*(4), 495–510. https://doi.org/10.1016/0012-821X(92)90127-H

Gislason, S. (2008). Weathering in Iceland. *Jokull*, *58*, 387–408.

Gislason, S. R., Arnorsson, S., & Armannsson, H. (1996). Chemical weathering of basalt in Southwest Iceland; effects of runoff, age of rocks and vegetative/glacial cover. *American Journal of Science*, *296*(8), 837–907. https://doi.org/10.2475/ajs.296.8.837

Grassa, F., Capasso, G., Favara, R., & Inguaggiato, S. (2006). Chemical and Isotopic Composition of Waters and Dissolved Gases in Some Thermal Springs of Sicily and Adjacent Volcanic Islands, Italy. *Pure and Applied Geophysics*, *163*(4), 781–807. https://doi.org/10.1007/s00024-006-0043-0

Halldórsson, S., Hilton, D., Scarsi, P., Abebe, T., & Hopp, J. (2014). A common mantle plume source beneath the entire East African Rift System revealed by coupled helium-neon systematics. *Geophysical Research Letters*, *41*. https://doi.org/10.1002/2014GL059424

Kaasalainen, H., & Stefánsson, A. (2012). The chemistry of trace elements in surface geothermal waters and steam, Iceland. *Chemical Geology*, *330–331*, 60–85. https://doi.org/10.1016/j.chemgeo.2012.08.019

Kebede, B. A. (2021). *The Relationship between the Tulu Moye Geothermal System, the Ziway–Asela Area and the Tectonic Structure of the Ethiopian Rift* [MS Thesis, Faculty of Earth Science, University of Iceland]. https://skemman.is/handle/1946/40002

Le Gall, B., Nonnotte, P., Rolet, J., Benoit, M., Guillou, H., Mousseau-Nonnotte, M., Albaric, J., & Deverchère, J. (2008). Rift propagation at craton margin.: Distribution of faulting and volcanism in the North Tanzanian Divergence (East Africa) during Neogene times. *Tectonophysics*, *448*(1), 1–19. https://doi.org/10.1016/j.tecto.2007.11.005

Lyu, H., Watanabe, T., Kilasara, M., & Funakawa, S. (2018). Effects of climate on distribution of soil secondary minerals in volcanic regions of Tanzania. *CATENA*, *166*, 209–219. https://doi.org/10.1016/j.catena.2018.04.005

Mahecha, A. (2019). *Structural control of north Tanzania volcanic area and its implication to geothermal fluid pathways; a case study of lake Natron and Meru volcano* [MSc Thesis]. Kyushu University.

Mahecha, A., Saadi, N., Watanabe, K., & Josephat, S. (2021). The quest for fluid pathways at Meru volcanic area, Tanzania, using remote sensing and soil gas analysis. *Proceedings World Geothermal Congress 2020+1*, 8.

Makoba, E., & Muzuka, A. (2019). Water quality and hydrogeochemical characteristics of groundwater around Mt. Meru, Northem Tanzania. *Applied Water Science*, *9*, 120. https://doi.org/10.1007/s13201-019-0955-3

Malago, J., Makoba, E., & Muzuka, A. N. N. (2020). Spatial Distribution of Arsenic, Boron, Fluoride, and Lead in Surface and Groundwater in Arumeru District, Northern Tanzania. *Fluoride*, *53*(2), 356–386.

Middelburg, J. J., van der Weijden, C. H., & Woittiez, J. R. W. (1988). Chemical processes affecting the mobility of major, minor and trace elements during weathering of granitic rocks. *Chemical Geology*, *68*(3), 253–273. https://doi.org/10.1016/0009-2541(88)90025-3

Mutonga, M. (2015). *Stable Isotopic Composition of Geothermal Fields in Kenya; The Relationship Between Geothermal Fields and Kenya Rift Lakes Waters*.

Nanyaro, J. T., Aswathanarayana, U., Mungure, J. S., & Lahermo, P. W. (1984). A geochemical model for the abnormal fluoride concentrations in waters in parts of northern Tanzania. *Journal of African Earth Sciences (1983)*, *2*(2), 129–140. https://doi.org/10.1016/S0731-7247(84)80007-5

Parkhurst, D. L., & Appelo, C. A. J. (1999). User's guide to PHREEQC (Version 2): A computer program for speciation, batch-reaction, one-dimensional transport, and inverse geochemical calculations. In *User's guide to PHREEQC (Version 2): A computer program for speciation, batch-reaction, one-dimensional transport, and inverse geochemical calculations* (USGS Numbered Series No. 99–4259; Water-Resources Investigations Report, Vols. 99–4259). U.S. Geological Survey. https://doi.org/10.3133/wri994259

Ranta, E., Halldórsson, S. A., Barry, P. H., Ono, S., Robin, J. G., Kleine, B. I., Ricci, A., Fiebig, J., Sveinbjörnsdóttir, Á. E., & Stefánsson, A. (2023). Deep magma degassing and volatile fluxes through volcanic hydrothermal systems: Insights from the Askja and Kverkfjöll volcanoes, Iceland. *Journal of Volcanology and Geothermal Research*, *436*, 107776. https://doi.org/10.1016/j.jvolgeores.2023.107776

Reed, M., & Spycher, N. (1984). Calculation of pH and mineral equilibria in hydrothermal waters with application to geothermometry and studies of boiling and dilution. *Geochimica et Cosmochimica Acta*, *48*, 1479–1492. https://doi.org/10.1016/0016-7037(84)90404-6

Roberts, M. A. (2002). *The Geochemical and Volcanological Evolution on the Mt. Meru Region, Northern Tanzania* [PhD Thesis]. Cambridge University.

Sharp, Z. (2017). Principles of Stable Isotope Geochemistry, 2nd Edition. *Open Textbooks*. https://doi.org/ https://doi.org/10.25844/h9q1-0p82

Tomašek, I., Mouri, H., Dille, A., Bennett, G., Bhattacharya, P., Brion, N., Elskens, M., Fontijn, K., Gao, Y., Gevera, P. K., Ijumulana, J., Kisaka, M., Leermakers, M., Shemsanga, C., Walraevens, K., Wragg, J., & Kervyn, M. (2022). Naturally occurring potentially toxic elements in groundwater from the volcanic landscape around Mount Meru, Arusha, Tanzania and their potential health hazard. *Science of The Total Environment*, *807*, 150487. https://doi.org/10.1016/j.scitotenv.2021.150487

Wayne Nesbitt, H. (1979). Mobility and fractionation of rare earth elements during weathering of a granodiorite. *Nature*. https://doi.org/10.1038/279206a0

White, W. M. (2020). *Geochemistry* (2nd Edition). Wiley Professional, Reference & Trade (Wiley K&L). https://www.wiley.com/en-us/Geochemistry%2C+2nd+Edition-p-9781119438052

Wilkinson, P., Mitchell, J. G., Cattermole, P. J., & Downie, C. (1986). Volcanic chronology of the Meru–Kilimanjaro region, Northem Tanzania. *Journal of the Geological Society*, *143*(4), 601–605. https://doi.org/10.1144/gsjgs.143.4.0601

Appendix

Table 1: Chemical composition of the nephelinites in the study area used for calculation of elemental relative mobility based on whole rock geochemistry. Data from (Roberts, 2002).

Major elements (wt-%)	
SiO_2	48.43
Al_2O_3	17.70
Fe_2O_3	8.76
FeO	6.30
MgO	2.32
CaO	6.46
Na_2O	8.30
K_2O	4.25
TiO_2	2.23
MnO	0.20
P_2O_5	0.55
Total	100.78
LOI	0.46
Trace elements (ppm)	
Ba	1630.29
Co	15.11
Cr	11.13
Cu	24.84
Ga	25.50
Hf	10.52
Nb	196.67
Ni	9.40
Pb	16.08
Rb	108.89
Sc	23.53
Sr	1669.76
Ta	10.19
Th	13.66
U	4.87
V	134.29
Y	39.16
Zn	118.07
Zr	476.90
REE (ppm)	
La	135.00
Ce	235.67
Pr	25.40
Nd	86.37
Sm	14.12
Eu	4.33
Gd	14.44
Tb	1.64
Dy	7.66
Ho	1.38
Er	3.87
Tm	0.51
Yb	3.09
Lu	0.44